filling methods which avoid flow of the feed particles down inclined heap surfaces.

Acknowledgment

The author is indebted to Mr. S. Takamatsu for help with experimental aspects and calculations and also to Dr. C. E. Capes for help with revisions of the manuscript.

Nomenclature

C = combination
d = particle diameter, cm
F = feed rate based on net volume of particles, cm^3/s
j,k = number of column and row corresponding to m and n in Table I, dimensionless
K = constant in flow rate equation through orifices
Δl = differential length of particle block along inclined heap line, cm
M = mixing ratio of nonspherical particles based on net volume of particles, dimensionless
m = number of differential block of particle feed, dimensionless
n = number of stationary zone where differential block is located, dimensionless
P = power of effective orifice diameter, dimensionless
Q = volumetric flow rate of nonspherical particles through interspaces of spherical ones per unit penetrating area of mixture, $cm^3\ s^{-1}\ cm^{-2}$
r = velocity ratio of nonspherical particles to flowing mixture along inclined heap line, dimensionless
Δt = differential time while each block stays in a zone, s
V = net volume of nonspherical particles supplied in each zone during Δt from above flowing layer of mixture by penetration, cm^3
v = velocity of particles flowing down on inclined heap surface, cm/s
$V_{b,n}$ = net volume of nonspherical particles left in flowing block of mixture in the nth zone, cm^3
w = distance between vertical sides of two-dimensional hopper, cm

Greek Letters

β = ratio of ineffective void which cannot be used for equivalent screen openings to effective void, dimensionless
ϵ = overall void fraction of particle mixture flowing down on solid heap, dimensionless
ρ = density of particle, g/cm^3
θ = cone angle of a hopper, deg

Subscripts

c = calcite particle
cr = critical zone
g = glass beads
i = initial
j,k = numbers of column and row corresponding to m and n
m,n = numbers of block and zone, respectively
t = total number of zones along heap surface

Literature Cited

Cheng, D. C.-H., Sutton, H. M., *Nature (London) Phys. Sci.*, **232**, 192 (1971).
Denburg, J. F., Bauer, W. C., *Chem. Eng.*, **71**, 135 (1964).
Hayashi, M., Suzuki, A., Tanaka, T., *Powder Technol.*, **6**, 353 (1972).
Shinohara, K., Shoji, K., Tanaka, T., *Ind. Eng. Chem. Process Des. Dev.*, **9**, 174 (1970).
Shinohara, K., Shoji, K., Tanaka, T., *Ind. Eng. Chem. Process Des. Dev.*, **11**, 369 (1972).
Shinohara, K., Hayashi, K., Tanaka, T., *J. Chem. Eng. Jpn.*, **6**, 447 (1973).

Received for review August 1, 1977
Accepted August 11, 1978

Power Consumption Studies of Helical Ribbon–Screw Mixers

Ranajit Chowdhury and Krishna K. Tiwari*

Department of Chemical Technology, University of Bombay, Matunga Road, Bombay-400019, India

Power measurements indicated that in the laminar flow regime the power (P) consumed during the agitation increased with speed of agitation (N) according to the relationship $P = K_1N^{1+n}$ where n is the flow behavior index and K_1 is a constant which depends on the assembly and fluid consistency index. For the helical ribbon–screw agitators, the constant k_s relating average shear rate in the mixer to the agitator speed ($\gamma = k_sN$) was found to be 30.6. Using this value of k_s and flow behavior index n, $PoRe$ and $PoRe'$ may be related as

$$PoRe' = K_p' = \frac{K_p}{(k_s)^{1-n}} = \frac{PoRe}{(k_s)^{1-n}}$$

The power consumption was found to be linearly proportional to the liquid depth.

Introduction

The helical agitators are used for processing high viscosity materials. The process may include blending of miscible liquids and accomplishing a chemical reaction involving heat and mass transfer. The helical agitators may be used in many diverse industries such as paints, plastics, synthetic fibers, rubber, petroleum, cosmetics, pharmaceuticals, foods, paper, and cement.

The efficiency of mixing is dependent upon the power input and the time for which the power is applied. A knowledge of both power consumption and mixing time is required in order to study a particular mixing operation. During the past 15 years, many research papers have appeared in the literature which give useful guidelines for selecting an agitator system for processing high viscosity materials. These studies indicate that the power consumption in the blending operation is much smaller when helical agitators are used as compared to the power consumed by turbines and propellers. Coyle et al. (1970) showed that for pseudoplastic fluids the mixing time is reduced when a helical screw is provided along with a ribbon on the same impeller shaft. Chavan and Ulbrecht

0019-7882/79/1118-0227$01.00/0

Table I. Dimensions of Assemblies

geometrical variable	assembly I	II	III	IV
impeller type	1R-3, S-3	1R-2, S-4	1R-3, S-3	1R-3, S-3
impeller diameter (d)	0.34 m	0.36 m	0.53 m	0.90 m
vessel diameter (D)	0.38 m	0.38 m	0.57 m	1.00 m
vessel volume	0.1 m^3	0.1 m^3	0.5 m^3	1.2 m^3
ribbon pitch to diameter ratio (p/d)	0.576	0.661	0.585	0.683
ribbon width to diameter ratio (w/d)	0.1027	0.0694	0.0943	0.0889
clearance to diameter ratio (c/d)	0.0588	0.0278	0.0377	0.0556
screw diameter to ribbon diameter ratio (d_s/d)	0.412	0.369	0.392	0.444
screw pitch to ribbon diameter ratio (p_s/d)	0.576	0.322	0.585	0.683
screw width to ribbon diameter ratio (w_s/d)	0.1618	0.1667	0.1604	0.2000
liquid depth to diameter ratio (h/d)	1	1	1	1
bottom clearance to diameter ratio (C_B/d)	0.118	0.056	0.075	0.111

(1973) found that the power consumption of a ribbon–screw impeller is almost the same as that of a ribbon impeller.

Bourne and Butler (1969) correlated their results for a single helical ribbon agitator to within ±15% with an equation based on the analytical solution for power consumption by fluid in the gap between coaxial cylinders whose diameters are the outer diameter of the ribbon and the inside diameter of the vessel. The correlation does not consider the effect of the ribbon width and the pitch of the ribbon on power consumption. Hall and Godfrey (1970) used five ribbon impellers in their experiments on power consumption. Their correlation takes into account the effect of pitch, ribbon width, and clearance between the agitator and the vessel wall. Nagata et al. (1972) presented data for three ribbon impellers and five ribbon–screw impellers. They correlated their data by considering the effect of pitch and the clearance between the ribbon impeller and the vessel wall. Chavan and Ulbrecht (1973, 1974) reported their results for a helical ribbon–screw impeller and presented a correlation for the power consumption of helical ribbon–screw impellers. The correlation uses the dimensions of the assembly such as the diameter, pitch, and width of the impeller, the height of the impeller immersed in the fluid, and the clearance between the impeller and vessel wall.

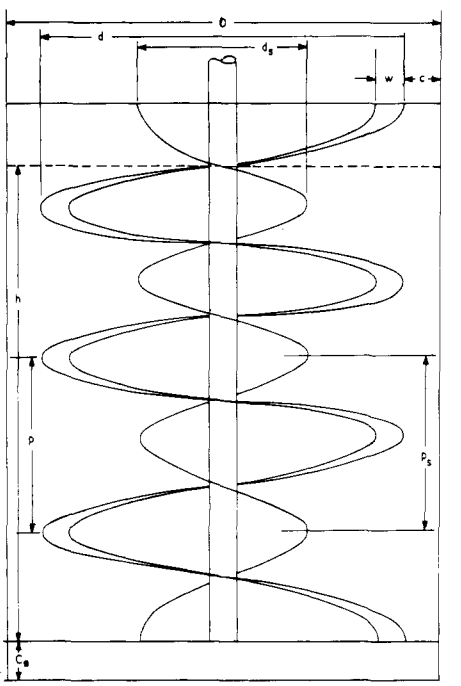

Figure 1. Geometry of the impeller (1R-3, S-3) and the vessel.

Experimental Section

For four different assemblies, the helical impellers contained a helical ribbon and a helical screw. The ribbon and screw were placed concentrically on the impeller shaft. The detailed geometries are shown in Table I. A schematic diagram of assembly (1R-3, S-3) is shown in Figure 1.

Gear box and four-step pulley arrangements were used to vary the speed of the agitator between 3 and 100 rpm for the first three assemblies. For the biggest assembly, a Kopp's variator with gear box arrangement was used to adjust the speed of agitator from 10 to 60 rpm.

The pseudoplastic fluids used were guar gum solutions (0.5%, 1.0%, 1.5%, 2.0%, 2.5%, 3.5%, and 4.5%) and CMC solutions (1%, 2%, 3%, 4%, and 5%). Newtonian liquid used was commercial grade glycerol. Guar gum and CMC solutions were prepared by adding powder to the bulk of the water heated by steam up to 60 °C in a jacketed anchor mixer of 0.2 m^3 capacity. Formaldehyde was added to the guar gum solution as a preservative in a quantity equivalent to 0.5% of the weight of the bulk guar gum solution. The rheological properties of these solutions were measured by a Stormer concentric cylinder viscometer and by a pipeline viscometer. Guar gum solutions up to 1% concentration did not show any viscoelastic behavior. Some climbing of the solution on the rotating inner bob of the Stormer viscometer was observed for guar gum solutions with concentrations of 1.5% and above. A typical plot of a shear rate vs. shear stress curve for 1% guar gum solution in the Stormer viscometer is shown in Figure 2. The rheological properties of different solutions are presented in Table II.

The power consumption was measured by using turntables of 0.68 m diameter for smaller assemblies and of 1.20 m diameter for the biggest assembly, respectively. The bearings used in the turntable had extremely low friction. The vessels were placed on these very low friction turntables. Due to the shearing action of the agitator and viscous liquid a torque of high magnitude was produced. This caused the vessel and turntable to rotate in the di-

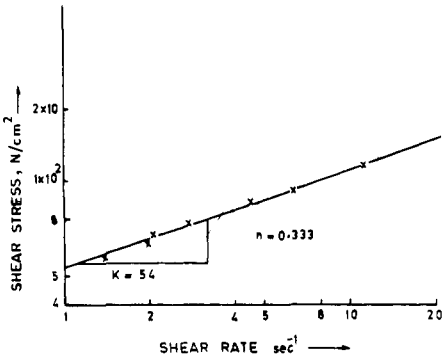

Figure 2. Relation between shear rate and shear stress for 1% guar gum using Stormer viscometer.

Table II. Rheological Properties of the Different Solutions Used

solution	consistency index K, N m^{-2} s^n	flow behavior index, n
0.5% guar gum solution	0.76	0.63
1% guar gum solution	5.4	0.33
1.25% guar gum solution	12.6	0.32
1.5% guar gum solution	16.62	0.31
1.75% guar gum solution	28.7	0.309
2% guar gum solution	34.4	0.30
2.5% guar gum solution	47	0.29
3.5% guar gum solution	83	0.275
4.5% guar gum solution	188	0.265
1% CMC solution	0.31	0.867
2% CMC solution	0.85	0.842
3% CMC solution	1.71	0.767
4% CMC solution	5.76	0.38
5% CMC solution	38.0	0.325
glycerol	0.23	1

rection of torque acted. The rotation was just checked by placing a load in the load pan hanging from a pulley at the periphery of the turntable. The power P was measured. The power P was calculated as

$$P = (W - w)2\pi rN \quad (1)$$

where W is the load (pan + load in the pan) required to balance the torque, w is the dead load required to overcome friction, and r is the radius of the turntable.

Results and Discussion

The power consumption data were taken for assembly I for 0.5%, 1.5%, 2.0%, 2.5%, and 3.5% guar gum solutions. Power consumption was measured for 2.5% and 3.5% guar gum solutions and 1% and 2% CMC solutions and commercial glycerol in assembly II. In assembly III, the power data were taken for 0.5%, 1.0%, 1.5%, 2.0%, and 4.5% guar gum solutions. In the biggest assembly, IV, 0.5%, 1.0% and 2.5% guar gum solutions and 5% CMC solution were used. Figure 3 shows the relation between power consumption and agitator speed in assembly I for different concentrations of guar gum solutions. Similar plots were obtained for power consumption in other assemblies.

The power measurements as shown in Figure 3 indicate that the power consumed during agitation increases with an increase in the speed of agitation. The relationship is of the type $P = \propto N^{\beta}$ where β depends on the solution. The plots of power consumption against agitator speed also indicate that in the range of speeds studied, the power consumption increases with an increase in viscosity of the solution at a particular speed and the slope decreases as one goes from the lower concentration to higher concentration. In the laminar region, the power number Po and Reynolds number Re' are related by the equation

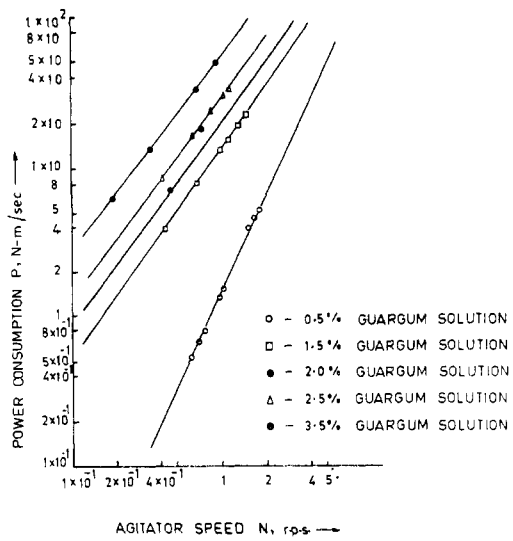

Figure 3. Relation between power consumption and agitator speed in assembly I.

$$Po = K_p'(Re')^{-1} \quad (2)$$

where

$$Po = \frac{Pg_c}{\rho N^3 d^5}; \quad Re' = \frac{\rho d^2 N^{2-n}}{K}$$

The constant of proportionality K_p' depends on the geometry of the assembly and the flow behavior index of the solution. From eq 2, a relationship between the power consumption P and agitator speed N of the following type is obtained for the laminar flow regime.

$$P = K_1 N^{1+n} \quad (3)$$

Here K_1 is a constant which depends on the geometry of the assembly and the properties of the solution. It was found that the slope of the lines on the log–log plot of P vs. N was very close to the value of $(1 + n)$ for only concentrated guar gum solutions (2% and above). For other solutions the slope of P vs. N lines was more than $(1 + n)$ because the lines for these solutions contained points in the nonlaminar region.

The power consumption was determined at three liquid depths, 0.27, 0.41, and 0.51 m, for agitator (1 R-2, S-4) in assembly II using 1.0% guar gum solution. The data for power consumption P vs. liquid depth h at several agitator speeds are presented in Figure 4. The straight lines indicate a linear relationship between power consumption and liquid depth in the range of agitator speed and liquid depth studied. At least one turn of ribbon was always immersed in the liquid in all experiments.

The data for power consumption vs. speed of agitation for different solutions obtained for all assemblies were converted into the form of power number versus Reynolds number (Re') data. These data were tabulated and plotted on log–log paper. From these, the data which gave a relationship of the type given by eq 2 were used to determine the values of K_p' for different solutions for each assembly. Some of these experimental values of K_p' are presented in Table III. It was found that as the concentration of guar gum or CMC solutions increased and the value of flow behavior index, n, decreased, the value of K_p' also decreased. It was also found that for the same concentration of guar gum solution, the value of K_p' was

Table III. Comparison of Experimental K_p and K_p' with Prediction from Correlations by Different Authors

	assembly	K_p	K_p' at $n = 0.31$	K_p' at $n = 0.29$	K_p' at $n = 0.275$
experimental values	I	190	19.9	15.0	13.6
	II	112		10.3	8.9
	III	221	20.8	20.1 (at $n = 0.3$)	19.0 (at $n = 0.265$)
	IV	176		15.6	
correlation of Nagata et al. (1972)	I	205	20.5	19.5	19.0
	II	274	27.3	26.0	25.3
	III	251	25.0	23.8	23.3
	IV	191	19.0	18.1	18.1
Hall and Godfrey (1970) correlation	I	175	17.4	16.7	16.2
	II	190	19.0	18.1	17.6
	III	216	21.6	20.4	19.4
	IV	147	14.6	14.0	13.4
Bourne and Butler (1969) correlation	I	190	19.0	18.0	17.6
	II	356	35.5	34.7	34.0
	III	275	27.3	26.2	25.5
	IV	207	20.5	19.6	18.6
Chavan and Ulbrecht (1973, 1974) correlation	I	203	20.2	19.3	18.9
	II	216	21.6	20.1	19.0
	III	252	25.2	23.8	22.2
	IV	190	18.9	17.9	17.6

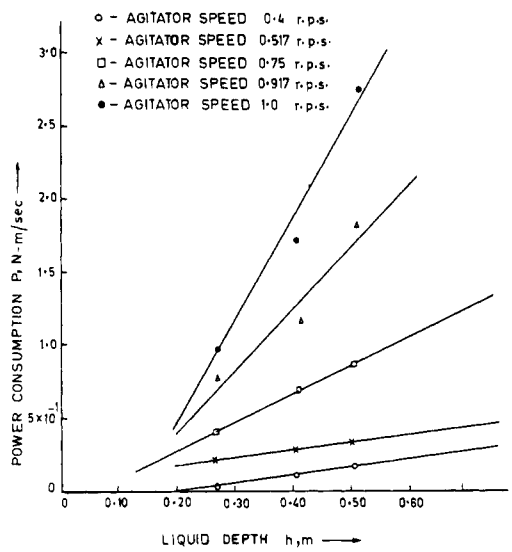

Figure 4. Relation between power consumption and liquid depth in assembly II for 1% guar gum solution.

highest for assembly III and lowest for assembly II.

The Reynolds number, Re ($= \rho d^2 N/\mu_A$), based on the apparent viscosity may be related, at least in the laminar region, to the Reynolds number Re' ($= \rho d^2 N^{2-n}/K$) by the equation

$$Re = Re'(k_s)^{1-n} \tag{4}$$

The equation is derived by assuming the fluids to be represented by the power law model and using the Metzner and Otto (1957) relationship between the average shear rate in an agitated vessel and the speed of agitation ($\dot{\gamma} = k_s N$). The data for Po vs. Re' for various solutions for each assembly, where the Re' were low enough for laminar flow conditions to prevail, were used to get a best fit value of the k_s from eq 4 so that the Po vs. Re plots on the log–log scale for all solutions fell on the same line. The values of k_s for assembly I through IV obtained in this manner are 31.4, 30.9, 29.8, and 30.4. The values of flow behavior index of the solutions used to get the k_s values varied between 0.38 and 0.265. Since the values are very close to each other, an average value of k_s equal to 30.6 may be used for helical ribbon–screw impeller. This value is very close to the value of 30 reported by Nagata et al. (1971), the value

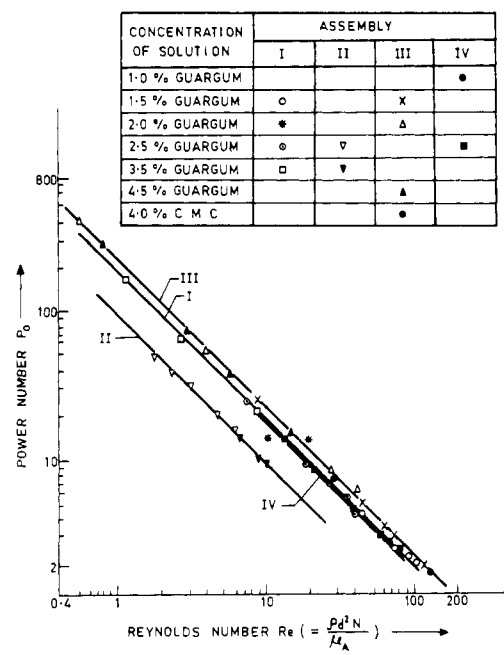

Figure 5. Power number vs. Reynolds number relationship in all assemblies.

of 27 reported by Hall and Godfrey (1970), and the value of 36.73 ± 1.45 reported by Rieger and Novak (1973).

The value of 30.6 for k_s obtained for helical ribbon–screw agitators was used to calculate the apparent viscosity, μ_A, from the flow curve (τ vs. $\dot{\gamma}$) determined from the viscometric data. The apparent viscosity was then used to calculate Reynolds number Re. The log–log plots of Po vs. Re for the four assemblies are shown in Figure 5. The plots indicate that a relationship of the type

$$Po = K_p Re^{-1} \tag{5}$$

exists in the laminar region up to a value of Reynolds number of approximately 100. This figure shows that the value of K_p is highest for assembly III and is lowest for assembly II. Out of the assemblies I, III, and IV having impellers of the type 1R-3, S-3 with three turns of ribbon and three turns of screw of which a length equal to diameter of ribbon of the impeller was immersed in the liquid, assembly III with the lowest clearance to diameter

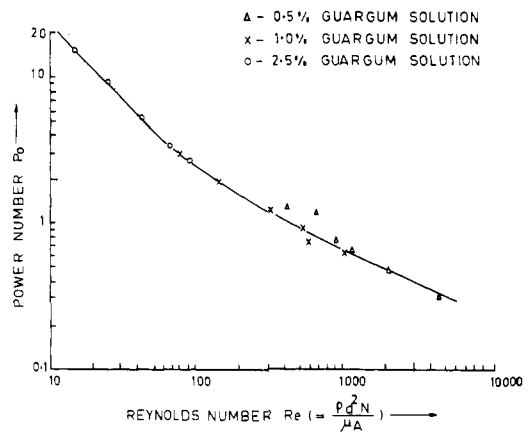

Figure 6. Relation between power number and Reynolds number in assembly IV.

ratio has the highest value of K_p. Assembly I, which has nearly the same clearance to diameter ratio as assembly IV but has a lower pitch to diameter ratio and higher ribbon width to diameter ratio, has a higher value of K_p of 190 in comparison to the K_p value of 176 for assembly IV. Assembly II, which has an impeller of the type 1R-2, S-4 having two turns of ribbon and four turns of screw, has the lowest value of K_p because of the low ribbon width to diameter ratio (0.0694).

The experimental values of K_p and K_p' and the values predicted by the correlations proposed by different authors are presented in Table III. From the table it is seen that the values of K_p and K_p' predicted by the correlations of Nagata et al. (1972), Bourne and Butler (1969), and Chavan and Ulbrecht (1973, 1974) are higher than the experimental values. The predicted values are within 15% of the experimental values except for assembly II where the predicted K_p and K_p' are very high. The values of K_p predicted by the Hall and Godfrey (1970) correlation are lower by about the same margin of 15% at the most except for assembly II where the predicted value is higher. Since assembly II has a much lower ribbon width to diameter ratio than the standard value of 0.1, the surface area is quite low. This in turn causes a lower power consumption but predicted K_p values are high. Although the value of K_p is low for assembly II, the value of k_s obtained for it is very close to the value obtained for other assemblies.

A typical plot of Po vs. Re extending into the transition region is presented in Figure 6. The experimental data suggest that in the transition regime the power consumption becomes a little lower as the concentration of guar gum solutions is increased for the same values of Reynolds number. The elasticity of the solution increases with an increase in concentration of guar gum solution. Thus the power consumption in the nonlaminar regime will be less for viscoelastic solutions than for inelastic solutions having the same consistency K and flow index n. This phenomenon has been reported by Kale et al. (1974) and by Ranade and Ulbrecht (1977) for disks and turbines, respectively.

Conclusions

The correlations of Nagata et al. (1972) and Chavan and Ulbrecht (1973) predict the K_p values to within 15% of the experimental values on the higher side. The values predicted by the Hall and Godfrey (1970) correlation are lower by about the same margin of 15% at the most. Since the prediction of a power consumption with higher value is always better than a lower value, the correlations of Nagata et al. (1972) or Chavan and Ulbrecht (1973, 1974) may be used to predict K_p. A better method, however, would be to determine P at any speed for the desired impeller when rotating in a solution of known rheological properties. From these data Po and Re' can be obtained. Since k_s equal to 30.6 may be assumed for all ribbon or ribbon–screw agitators as seen from the present work, the value of K_p' for the agitation of any fluid may be found. This may then be used to determine the power at any operating condition, as long as the flow is in the laminar regime. When working with nonstandard geometries as in the case of assembly II, the K_p cannot be predicted by any proposed correlation. In such a case the value of K_p and K_p' must be obtained experimentally. Again, a value of k_s equal to 30.6 may be used to obtain power consumption data at any other operating condition.

Nomenclature

d = diameter of the impeller (outer diameter of the helical ribbon), m
g_c = conversion factor, kg m/N s^2
h = liquid depth in agitated vessel, m
K = consistency index in the power law model, N m^{-2} s^n
k_s = proportionality constant between average shear rate and the rotational speed of the agitator
K_p = proportionality constant of power number and Reynolds number ($\rho d^2N/\mu_A$) correlation in laminar regime
K_p' = proportionality constant of power number and Reynolds number ($\rho d^2N^{2-n}/K$) correlation in laminar regime
K_1 = proportionality constant of power vs. agitator speed in laminar regime in eq 3
n = flow behavior index in the power law model
N = rotational speed of the impeller, revolutions per second
P = power consumption, N-m/s
r = radius of the turntable, m

Greek Letters

α = proportionality constant in the correlation of power vs. agitator speed
β = exponent of agitator speed in the correlation of power vs. agitator speed
$\dot{\gamma}$ = shear rate, s^{-1}
μ_A = apparent viscosity, N s m^{-2}
ρ = density, Kg$_m$/m^3

Dimensionless Number

Power number $Po = Pg_c/\rho N^3 d^5$
Reynolds number $Re' = \rho d^2 N^{2-n}/K$
Reynolds number $Re = \rho d^2 N/\mu_A$, based on average shear rate

Literature Cited

Bourne, J. R., Butler, H., *Trans. Inst. Chem. Eng.*, **47**, T263 (1969).
Chavan, V. V., Ulbrecht, J., *Ind. Eng. Chem. Process Des. Dev.*, **12**, 472 (1973); Correction, **13**, 309 (1974).
Coyle, C. K., Hirschland, H. E., Michel, B. J., Oldshue, J. Y., *AIChE J.*, **16**, 903 (1970).
Gray, J. B., *Chem. Eng. Prog.*, **59**, No. 3, 55 (1963).
Hall, K. R., Godfrey, J. C., *Trans. Inst. Chem. Eng.*, **48**, T201 (1970).
Kale, D. D., Mashelkar, R. A., Ulbrecht, J., *Chem. Ing. Tech.*, **46**, 69 (1974).
Metzner, A. B., Otto, R. E., *AIChE J.*, **3**, 3 (1957).
Nagata, S., Nishikawa, M. Tada, H., Gotoh, S., *J. Chem. Eng. Jpn.*, **4**, 72 (1971).
Nagata, S., Nishikawa, M., Katsube, T., Takaish, K., *Int. Chem. Eng.*, **12**, 175 (1972).
Ranade, V. R., Ulbrecht, J., Proceedings, 2nd European Conference on Mixing, Cambridge, 1977.
Rieger, F., Novak, V., *Trans. Inst. Chem. Eng.*, **51**, T105 (1973).

Received for review August 16, 1977
Accepted July 26, 1978